Published in Surface Science 492, issue 3, 294-304, 2001
which should be used for any reference to this work

Oxidation of Al–Pd–Mn quasicrystal surfaces

D. Popović *, D. Naumović, M. Bovet, C. Koitzsch, L. Schlapbach, P. Aebi

Institut de Physique, Université de Fribourg, Pérolles, CH-1700 Fribourg, Switzerland

Abstract

The oxidation of both, quasicrystalline and crystalline surfaces of an icosahedral Al–Pd–Mn quasicrystal cut perpendicular to its five-fold axis and of Al(1 1 1) has been studied by means of X-ray photoelectron spectroscopy, ultraviolet photoemission spectroscopy, low-energy electron diffraction and X-ray photoelectron diffraction. The oxidation of the elements of the alloy is quantified and compared for the different phases and Al(1 1 1). The quasicrystalline surface is found to react less with oxygen than the crystalline surface and more rapidly compared to Al(1 1 1). The observed behaviour is discussed in terms of the termination of the corresponding surfaces.

Keywords: Oxidation; Alloys; Aluminum; Photoelectron spectroscopy

1. Introduction

Quasicrystals are well-ordered metal alloys with no translational symmetry. This unusual property attracts the attention of fundamental research. On the other hand, quasicrystals offer some interesting features for applications, such as low coefficient of friction, low surface energy, high electrical resistivity and hardness, but low thermal conductivity [1–3]. The possibilities for applications have initiated the investigation of the oxidation of quasicrystal surfaces.

Both, crystalline (c-) and quasicrystalline (qc-) surfaces can be prepared on the bulk icosahedral (*i*-) Al–Pd–Mn quasicrystal by specific sputtering and annealing treatment [4,6]. From previous work [7–9] it is known that the qc-Al–Pd–Mn surfaces oxidise in a two-step process (chemisorption of oxygen followed by oxide formation), forming a thin, passivating and spatially inhomogeneous oxide layer. The oxidation resembles that of elemental Al. Thin oxide layers (5 Å) form under ultra-high vacuum (UHV) conditions. Thicker layers grow (up to 100 Å) if the oxygen exposure is performed in a more aggressive environment [8,9]. Previous work [7–9] also reported that Al is the only element to oxidise and segregate at the surface whereas the other elements of the alloy appear to oxidise only in the presence of water [8–10]. Saturation of the oxidation process is reported at exposures around 50 L [7] or 80 L [8,10,11] (1 Langmuir (L) = 10^{-6} Torr s) and oxidation is pressure dependent [12]. Low-energy electron diffraction (LEED) spots disappear at 20–25 L [7], indicating the destruction of the long-range order. The surface energy and the friction

* Corresponding author. Tel.: +41-26-300-9088; fax: +41-26-300-9747.

E-mail address: dunja.popovic@unifr.ch (D. Popović).

coefficient of the oxidised quasicrystalline surface are lower than for Al-oxide and make quasicrystals attractive for surface coating applications [2].

In the c-surface, oxidation of Mn [11] and Pd [10] occurs as well. It is reported that Al enrichment of the surface is weaker in the c-phase than in the qc-phase [10], but that the oxidation is stronger [3]. Larger amounts of aluminium and almost all manganese at the surface are oxidised and thicker oxides are formed [3,10].

The study of oxidation has also been performed on other quasicrystals, such as Al–Cu–Fe [10,11, 13–15].

Upon exposure to oxygen, elemental Al forms a protective, passivating, amorphous oxide layer [16,17]. The LEED pattern disappears at exposures of the order of 1000 L for the close-packed (1 1 1) face and at one order of magnitude smaller exposures for (1 1 0) and (0 0 1) faces [16,18,19]. The latter immediately develop bulk-like oxide films, because of their more open geometry, whereas the (1 1 1) face goes through a two-step oxidation (chemisorption of oxygen followed by oxide formation) [16,20,21]. In a high-resolution synchrotron-radiation study five different peaks appear in the Al 2p X-ray photoelectron spectroscopy (XPS) line of the Al(1 1 1) surface exposed to oxygen [16]. The substrate core levels shift due to the charge transfer between oxygen atoms and the substrate [22]. Two peaks in the valence band of Al(1 1 1) appear at 7.1 and 9.8 eV below the Fermi edge, related to the O 2p orbitals perpendicular (σ) and parallel (π) to the surface, respectively [19]. The transformation of the second peak into a continuum of states signalises the formation of the oxide [23]. The oxidation of Al(1 1 1) is a pressure-dependent process [24] and differences exist between oxidation in pure oxygen or water [20,25].

The aim of this work is to quantify the differences between the oxidation of quasicrystalline and crystalline surfaces of *i*-Al–Pd–Mn in pure oxygen and to characterise the changes upon exposures to oxygen using different techniques, i.e., XPS, X-ray photoelectron diffraction (XPD), ultraviolet photoemission spectroscopy (UPS) and LEED. The Al–Pd–Mn qc-surface is Al-rich [26,27] and, in order to examine the similarities with the oxidation of Al, an Al(1 1 1) crystal was used in the oxidation experiments for comparison.

2. Experimental

The *i*-Al–Pd–Mn quasicrystal ingot has been grown using the Czochralsky method in CECM–CNRS, Vitry-sur-Seine, France. It has been polished with diamond paste and oriented with its five-fold axis normal ($\pm 3°$) to the surface. Its stoichiometry was determined to be $Al_{70.3}Pd_{21.4}Mn_{8.3}$. The shape of the sample is a half disk, 2 mm thick and more than 10 mm in diameter. The qc-surface is a bulk-terminated icosahedral surface prepared by sputtering and annealing [6]. The c-surface can be interpreted as five domains of a cubic bcc Al–Pd crystalline alloy oriented perpendicularly to its [1 1 3] direction [5] and is prepared on the *i*-Al–Pd–Mn by Ar^+ sputtering without annealing [6].

Contamination-free surfaces were obtained by successive cycles of Ar^+ sputtering at 0.5–1.5 kV and annealing during approximately 15 min. The annealing temperature was controlled with a pyrometer. For the qc-Al–Pd–Mn surface the annealing temperature was 620°C and for Al(1 1 1) 500 °C. For c-Al–Pd–Mn the surface was not annealed [6]. The cleanliness of the surface was checked with UPS [22] and cleaning cycles were repeated until no features on the position of O 2p derived states were observed. LEED was used to check the surface ordering for the qc-surface and Al(1 1 1). Compositions were determined with cross-section corrected XPS core-level peak areas. The XPD patterns served for near-surface geometrical structure analysis. [1] Oxidations have been performed at 1×10^{-8} mbar for exposures smaller than 10 L; 5×10^{-8} mbar for medium exposures and 7×10^{-8} mbar for exposures larger than 100 L.

[1] The emitted photoelectron wave from a chosen core-level scatters at the surrounding atoms and interferes with the directly emitted wave to give an interference pattern as a function of emission angle. This strongly anisotropic angular distribution of photoelectrons then gives the possibility to obtain a basic picture of the local, real-space environment of the emitter, due to the "forward focusing" phenomenon. (For a detailed review on XPD, see e.g., Ref. [28].)

Oxygen was supplied by back-filling the preparation chamber through a leak valve. The exposure values in units of Langmuirs are not calibrated to the sensitivity of the pressure gauge.

The experimental set-up represents an extended version of the Vacuum Generators ESCALAB Mk II spectrometer, operating with a base pressure in the low 10^{-10} mbar region. XPS, XPD and UPS have been performed in the analysis chamber, equipped with a twin-anode X-rays source, an ultraviolet (UV) lamp with monochromator [29] and a hemispherical electron-energy analyser with a three-channeltron detection system. A motorised manipulator allows sample rotation with two degrees of freedom. All the measurements were carried out at room temperature. XPS and XPD (not shown) were performed with Mg Kα ($h\nu = 1253.6$ eV) radiation. The spectra have been measured with a pass energy of 50 eV corresponding to an energy resolution (Mg Kα source and analyser) of approximately 1 eV. Normal emission or 45° off-normal emission was used for the X-ray spectra, as will be indicated. The 45° off-normal geometry is more surface sensitive. For technical reasons the Al(1 1 1) surface has only been measured at normal emission. In order to have a quantitative comparison, some of the experiments on Al–Pd–Mn have been performed at normal and 45° off-normal emission. Monochromatised He I radiation ($h\nu =$ 21.2 eV) was used in UPS. All UPS measurements were performed at normal emission. LEED patterns (not shown) were recorded with normal incidence and electron energies of 60 eV.

3. Results and discussion

3.1. XPS

The compositions for the clean surfaces of the qc- and the c-phase are determined by XPS to be 68.5% Al, 27% Pd and 4.5% Mn and 58.8% Al, 36.7% Pd and 4.5% Mn, respectively. The qc-phase displays the characteristic features of the quasicrystals: five-fold symmetry (as seen from XPD) and a pseudogapped Fermi edge (as seen from UPS), while the crystalline surface has a metallic character (as seen from UPS) [4,6]. The core-level lines of Al and Mn in the qc-phase lie close to their positions in the elemental samples, while the Pd lines are 2 eV shifted towards higher binding energies compared with the ones of elemental Pd [8,9]. The lines of Al and Mn are at the same positions for the qc- and the c-surface of Al–Pd–Mn, while the positions of Pd lines at the c-surface are less shifted towards higher binding energies (<1 eV shift) than in the qc-phase. This is consistent with the reported changes from pure elements to the alloy [8,9]. In the valence band of the alloy, the Pd 4d derived feature is at 4.3 eV below the Fermi edge for the qc-surface, but at 3.7 eV binding energy in the crystalline phase, and the shift is in the same direction as described for the core-levels.

Changes of the core-level spectral lines upon exposure to oxygen are presented in Fig. 1a–d. The vertical arrows indicate oxygen exposure values, A corresponding to 0, 10, 35, 75, 110 L at 45° off-normal emission and B to 0, 20, 75, 150, 225, 300, 375 L at normal emission (sequences from bottom to top). For graphs with results of the qc-phase, exposure to 8400 L at 45° off-normal emission is presented by spectra in grey. The results of a quantitative analysis are shown in Fig. 2.

In Fig. 1a oxidation-induced changes characteristic for the Al 2p emission appear in the spectra of c-, qc-Al–Pd–Mn and Al(1 1 1) surfaces. A second peak appears and grows as a shoulder on the higher binding-energy side of the initial Al 2p peak, which decreases in intensity due to oxygen coverage. The Al 2s peak shows the same behaviour (not shown). As can be seen from the growth in intensity of the shoulder with oxygen exposure, Al oxidises less in Al(1 1 1) (Fig. 1a, bottom) than in qc-Al–Pd–Mn (Fig. 1a, middle), but less in qc-Al–Pd–Mn than in c-Al–Pd–Mn (Fig. 1a, top). Spectra presented in Fig. 1a are taken at 45° off normal for c-Al–Pd–Mn, where the measurement is more surface sensitive and at normal emission for qc-Al–Pd–Mn and Al(1 1 1), but the same conclusions follow from the examination of spectra taken at 45° off-normal emission (not shown) for both Al–Pd–Mn surfaces. In addition, exposures B consist of significantly higher doses than exposures A.

The Al 2p line has been fitted by a linear combination of the metallic emission peak, a Gaussian representing the appearing oxygen-related peak

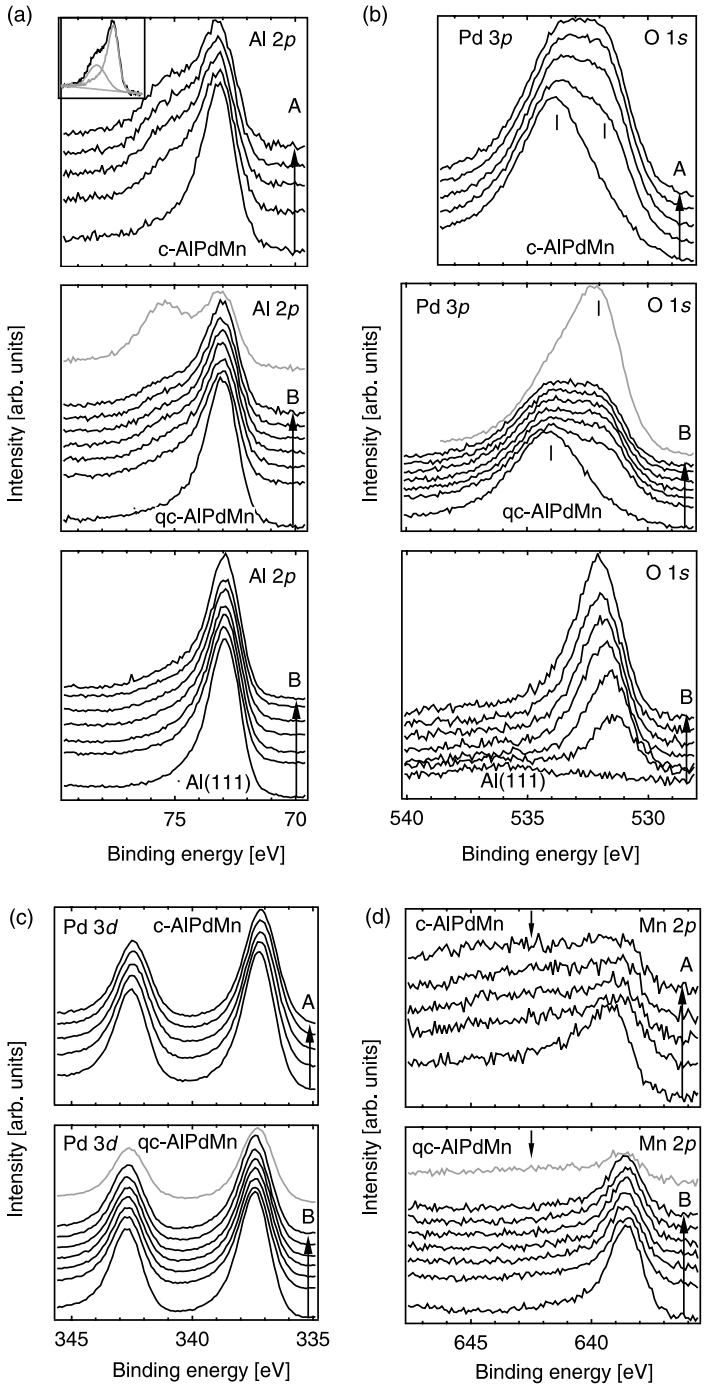

Fig. 1. XPS spectra of (a) Al 2p, (b) Pd $3p_{3/2}$ and O 1s, (c) Pd 3d and (d) Mn $2p_{3/2}$ core-level emission from qc-, c-Al–Pd–Mn and Al(1 1 1). The arrows are indicating oxygen exposure values: A: 0, 10, 35, 75, 110 L at 45° off-normal emission and B: 0, 20, 75, 150, 225, 300, 375 L at normal emission (sequences from bottom to top). Exposure of 8400 L is performed at 45° off-normal emission and presented in grey. The inset shows a typical fitting in the case of Al 2p (c-Al–Pd–Mn at 110 L of O_2 exposure).

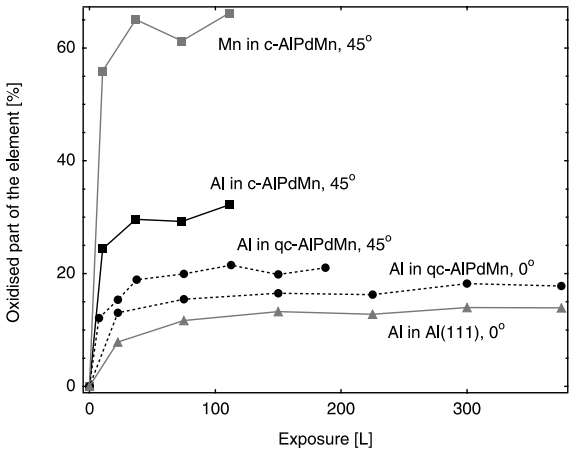

Fig. 2. Percentages of oxidised Al (Mn) in total amount of Al (Mn) atoms. Surfaces as indicated. The Al(1 1 1) surface has only been measured at normal emission and results on Al–Pd–Mn at both normal and 45° off-normal emission are presented in order to have a quantitative comparison with both c-Al–Pd–Mn and Al(1 1 1).

and a linear function, representing the linear background of the fitted spectrum (the inset in Fig. 1a presents a result for oxidised c-Al–Pd–Mn). The Al 2p peak of the clean surface has an asymmetrically-broadened form, characteristic for metals [22,30]. The linear-background subtracted spectrum of the clean surface was used to represent the metallic substrate emission. The underlying idea that its shape remains unchanged during the oxidation, has been also applied in other fitting procedures [25,31].

For the estimation of the growth of the oxygen/oxide layer the investigation of the O 1s peak was performed (Fig. 1b). O 1s and Pd $3p_{3/2}$ are energetically very close (Fig. 1b, top and middle) and each spectrum was fitted with the metallic Pd $3p_{3/2}$ peak, a Gaussian shape for O 1s and a linear background. The linear-background subtracted spectrum of the clean surface was used as Pd $3p_{3/2}$ peak in the fitting. O 1s spectra on the Al(1 1 1) surface (Fig. 1b, bottom) were fitted with a Gaussian function and a linear background. All parameters used in the fitting procedures throughout this work were variable.

Concerning the Pd 3d lines, it is known from previous work [8] that, upon oxidation, elemental palladium 3d lines broaden and shift towards higher binding energies. The position of the palladium lines in the qc-surface is already shifted by 2 eV towards higher binding energies with respect to the position of elemental palladium, and according to Ref. [9] the expected oxidation-induced shift is towards lower binding energies for the qc-surface.

In Fig. 1c we observe a decrease of the total intensity of the Pd 3d line of the Al–Pd–Mn surfaces with increasing exposures to oxygen. This signalises that, due to the growing coverage of the oxygen/oxide, the Pd signal from the alloy declines. A shift, smaller than 0.2 eV, towards lower binding energies can be noticed, more pronounced in the crystalline phase. According to Ref. [9], this is expected for the oxidised surface, but is not in agreement with reported results [8], where a shift of 0.1 eV towards higher binding energies is measured. We observe no changes of the spectral-line widths or asymmetries. The latter indicates that the palladium density of states near the Fermi level does not change significantly and that there is consequently no change of the environment related to oxygen bonding [32]. The Pd 3d shift could also indicate a change of environment due to the oxidation of other elements in the alloy. If palladium oxidises, the proportions of this effect are quite weak: a small shift is observed, but no spectral-line broadening. This is in agreement with the previously found inertness of pure metallic palladium [8]. The changes of Pd lines in qc- and c-Al–Pd–Mn surfaces are comparable and the claim of oxidation in one case would have to apply to the other as well, contrary to the reported oxidation of Pd only in the c-phase [10].

Mn in qc-Al–Pd–Mn does not oxidise for exposures up to 375 L, the metallic emission simply decreases, like in the case of Pd (Fig. 1d, bottom). The spectra along the B arrow all show absence of features on the higher binding-energy side of the metallic peak (Fig. 1d, bottom). Line shifts or changes in the line shape have not been noticed. In c-Al–Pd–Mn Mn oxidises to a very high extent: the metallic Mn line declines in intensity and another peak grows on its high binding-energy side from the lowest exposures (Fig. 1d, top, arrow points at the oxygen-induced peak). The same analysis procedure as described for Al 2p (Fig. 2) was applied in this situation.

Spectra in grey (Fig. 1) show that upon exposure of qc-Al–Pd–Mn to 8400 L of oxygen, Al oxidises to a great extent (Fig. 1a, middle), O 1s peak grows correspondingly (Fig. 1b middle), signs of oxidation of Mn are visible (Fig. 1d, bottom) and Pd 3d shifts more than for the moderate exposures (Fig. 1c, bottom). Mn has been considered not to oxidise at all under UHV at room temperature and not even after exposure to air (if not very humid) [8–10]. We show unambiguously that oxidation of Mn happens even in UHV at room temperature, for extremely large exposures (Fig. 1d, bottom, spectrum in grey). The arrow points at the oxygen-related feature appearing in the same way as for the c-surface (Fig. 1d, top). Note, that the spectral shape in the region of the arrow changes from a downward to an upward curvature upon oxidation.

In Fig. 2 we present how the percentage of the element which is oxidised, within the probing depth, changes with exposure. The percentage of the element which is oxidised is calculated as the ratio of the oxidation-induced shoulder area and the total peak area. Quantitative analysis (Fig. 2) confirms our observations of the changes visible in the raw spectra (Fig. 1). More than 50% of Mn oxidises in the c-Al–Pd–Mn, exceeding percentages of oxidised Al in both Al–Pd–Mn phases. Al also oxidises more in the crystalline than in the quasicrystalline phase. Finally, Al oxidises more in the alloy than in Al(1 1 1), a fact that is not merely a consequence of our probing depth. The Al density in the volume probed with XPS of the Al(1 1 1) surface is homogeneous. The structure of the qc-surface of Al–Pd–Mn is described in the model by Gierer et al. [26,27], which is based on the bulk structure proposed by Boudard et al. [33] and de Boissieu [34]. In the profile of the qc-surface in this model, there are four different types of layers and three of them contain aluminium. Within the first 5 Å there are eight layers and only one of them without aluminium. This distribution continues down to 20 Å depth, which means that the distribution of Al is also homogeneous at this scale, as in the bulk of the quasicrystal. The same holds for the c-Al–Pd–Mn, since its periodic structure guarantees uniform distribution of atoms of different elements on the scale of the order of 10 Å (mean free path of XPS) or more. The fact that we do not probe only the topmost Al-rich layer of the qc-surface and that all the surfaces have a uniform composition at the relevant depth scale, enables the comparison of the quantity of oxidised Al among the different surfaces examined.

The XPD pattern taken at the oxygen $KL_{23}L_{23}$ Auger transition line (not shown) does not display any anisotropy. This confirms the formation of a disordered oxide. XPD patterns of the clean c-surface show anisotropy characteristic for its specific structure [6]. Upon exposure to oxygen, these patterns become blurred for the Al and Pd emission, but visible up to the highest exposures. No image anisotropy is seen for the Mn emission on the crystalline surface after 110 L oxygen exposure, which is consistent with the high degree of oxidation of this element in the crystalline phase.

The alloy composition (Fig. 3) has been calculated to yield 100% for Al, Pd and Mn, while the percentage of O adds to that. Surface segregation of Al occurs in both Al–Pd–Mn phases (Fig. 3a) and segregation of Mn occurs in c-Al–Pd–Mn (Fig. 3b). The contribution of Pd is decreasing in both phases (Fig. 3c), as well as Mn in the quasicrystalline phase (Fig. 3b). The compositions of the clean qc-Al–Pd–Mn and c-Al–Pd–Mn are different, but relative changes are stronger in the crystalline phase (Fig. 3). The percentage of Pd (Fig. 3c), for instance, changes by less than 10% in the quasicrystalline phase subjected to exposures up to 375 L; for the crystalline phase this change is 15% for exposure of 110 L. It is known that the diffusivity of specific elements in the quasicrystals is at least one order of magnitude smaller than the diffusivities of elemental samples of its components [35]. The diffusivity in the crystalline phase is also larger than the one of the quasicrystalline phase [36]. This is consistent with the noticed line-position changes in these phases from the beginning of Section 3.1, suggesting that the properties of the crystalline phase are between the ones of the quasicrystal and the elemental crystals. Thus we observe stronger segregation in the c-Al–Pd–Mn than in the qc-Al–Pd–Mn. Both percentages of Al and Mn have increased in the crystalline surface during the oxidation process, but the relative increase of Mn is larger. The heats of formation of

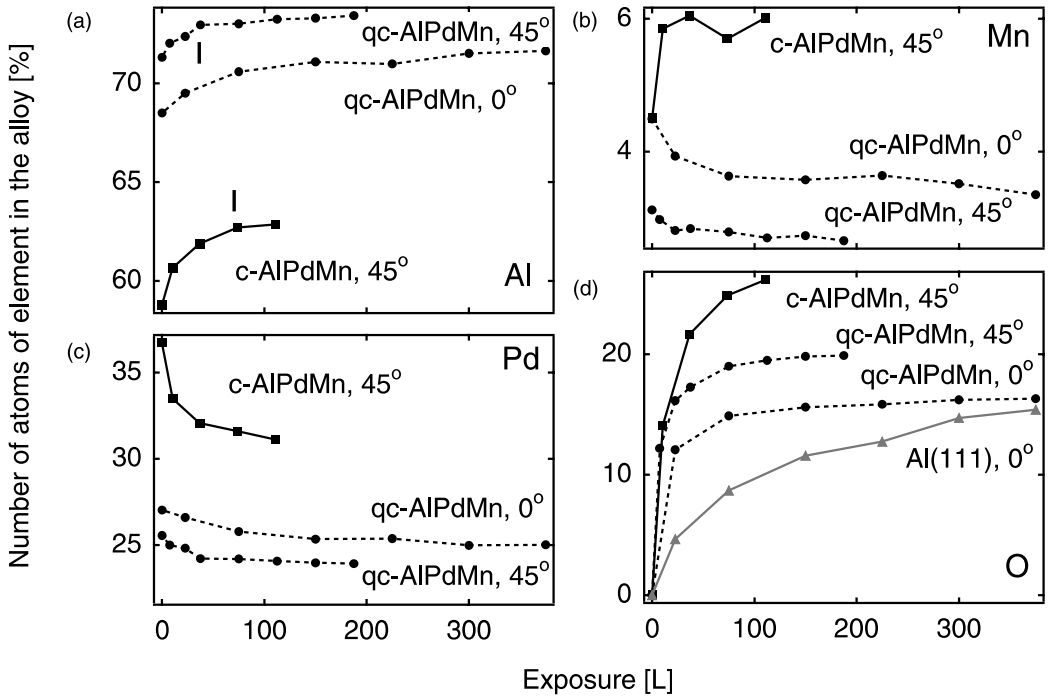

Fig. 3. Number of atoms of (a) Al, (b) Mn, (c) Pd and (d) O in oxidised surfaces. Percentages of the first three add up to 100. Percentage of O is given in addition of the clean sample 100% and as the percentage of clean sample total atoms. Markers are indicating the saturation points: 40 L for the qc-Al–Pd–Mn and 75 L for the c-Al–Pd–Mn. Surfaces as indicated.

the bulk oxides of Al and Mn are −1676 to −1657 kJ/mol for Al_2O_3 and −1388 kJ/mol for Mn_3O_4, respectively, much larger than −85 kJ/mol for PdO [37]. This explains why both Al and Mn strongly oxidise and segregate at the surface, contrary to the behaviour observed in the quasicrystalline phase.

It is important to notice that a layer-by-layer compositional structure as in the case of the qc-surface, with the exponential decay of XPS sensitivity with depth in the substrate, would not show any significant surface segregation effect if only a coverage of oxygen (lower than 15 Å, which is the case in our experiment) is added on top. This goes along with the discussed homogeneous distribution of the elements on the scales of the order of 20 Å and the XPS mean free paths that are certainly above 5 Å. The observed XPS intensity changes can only be explained by significant segregation, i.e. diffusion of Al, which is confirmed by the observed Al-oxide formation. It is difficult to conclude whether diffusion of Al only from the topmost two layers of the qc-surface into the oxygen overlayer is sufficient to give the observed rate of Al-segregation, or whether the diffusion of atoms from deeper layers in the qc-surface is needed.

The increasing percentage of oxygen, added to exceed the 100% of the clean-sample composition, is shown in Fig. 3d. The amount of oxygen in the crystalline phase is the largest. The oxygen percentage in Al(1 1 1) grows slower and remains below the one in qc-Al–Pd–Mn, approaching the value at which the quasicrystal has saturated. A calculation of the sticking coefficient for the clean surface [2] gives a six times larger value for the quasicrystal than for Al(1 1 1).

The composition changes in Al–Pd–Mn saturate approximately around 75 L in the crystalline

[2] The determination of the sticking coefficient is described in Ref. [38].

and around 40 L in the quasicrystalline phase (Fig. 3), consistent with the previous results [7–9]. The saturation values are marked in Fig. 3a, where it is best seen.

The positions of oxygen-related peaks are shifting towards higher binding energies with increasing exposures, as determined from the fitting procedure. The Pd 3d doublet shifts towards lower binding energies. In both, qc-Al–Pd–Mn and Al(1 1 1) the final position of O 1s is 532 eV and that of the Al 2p shoulder is 75.2 eV, in agreement with the literature values for Al_2O_3 on Al(1 1 1) [20,25]. Shifts of the Al and Mn oxygen-induced shoulders are more pronounced in the crystalline phase, consistent with the larger oxygen uptake in this phase.

3.2. UPS

Upon exposure to oxygen O 2p derived features appear in the valence band region of Al(1 1 1) and the Al–Pd–Mn surfaces (Fig. 4a–c). They consist of one main peak, around 7 eV binding energy, and a shoulder on the higher binding-energy side, at approximately 9 eV below the Fermi edge, in agreement with the literature values for oxygen on Al(1 1 1) [19]. The palladium feature in the valence band of Al–Pd–Mn surfaces (~4 eV binding energy) becomes attenuated with increasing exposure (Fig. 4a and b). Fig. 4 shows that the structure of the O 2p peak is slightly different for different surfaces: it grows narrower on Al(1 1 1) (Fig. 4c), broader on qc-Al–Pd–Mn (Fig. 4b) and even broader on c-Al–Pd–Mn (Fig. 4a). This is probably related to the number of peaks involved in the oxygen structure and their corresponding parameters. The Fermi level intensity of the surfaces investigated decreases with the exposure.

For a quantitative analysis, the clean-surface valence band was subtracted from every valence band spectrum and the area of the oxygen feature (peak 1, positive) and the area which is taken away from the palladium feature (peak 2, negative) were calculated (Fig. 4d). Oxygen grows more and palladium declines more in the crystalline than in the quasicrystalline phase (Fig. 4d). The changes of the peak areas with exposure are monotonic and consistent for both peaks. Therefore the conclusion about the more pronounced oxygen-induced changes in the crystalline phase is feasible, regardless of possible photon intensity variations for spectra taken at different exposures. Furthermore, the changes in the valence band approach saturation at the same exposures, as in XPS.

3.3. Sensitivity to photon irradiation

Another important point to notice is that X-rays and UV light promote the oxidation of the surfaces studied in this work. This has been tested by exposing the given surface to X-rays, UV light

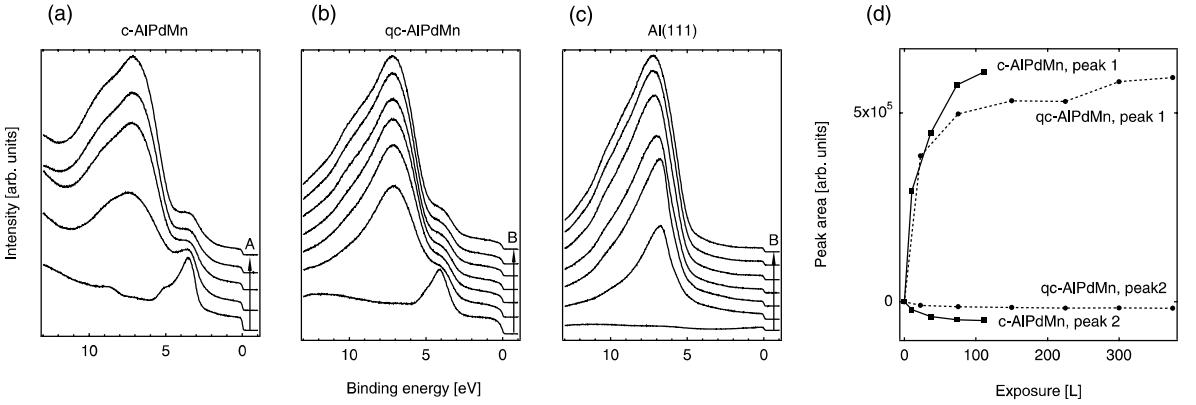

Fig. 4. UPS spectra of (a) c-, (b) qc-Al–Pd–Mn and (c) Al(1 1 1). The arrows are indicating oxygen exposure values, A: 0, 10, 35, 75, 110 L and B: 0, 20, 75, 150, 225, 300, 375 L (sequences from bottom to top, measured at normal emission). Peak area analysis is presented in (d).

or just by leaving it in UHV for approximately 1 h. Tests have been performed on the clean surfaces, on the surfaces oxidised with 15 L of oxygen and on the highly oxidised quasicrystalline surface exposed to 8400 L of oxygen. UPS was used to detect the quantity of oxygen present on the surface before and after the treatment, since it is more sensitive than XPS.

All surfaces examined show stronger changes after photon irradiation than by merely keeping them in UHV. A similar result for Al(1 1 1) has already been reported [39]. On the qc-surface all these changes are stronger than on both the c-Al–Pd–Mn and the Al(1 1 1) surfaces.

The described effects are more pronounced at the surfaces previously exposed to oxygen. This is illustrated in Fig. 5 for the qc-surface. Upon exposure to UV light during 1 h the valence band spectrum of the clean qc-surface (bottom) changes less than the one of the oxidised surface (top). In the extreme case of 8400 L exposure the effects are of the same magnitude as for the ones oxidised with 15 L of oxygen.

It has been suggested by Cabrera and Mott [39] that an increased oxidation in the presence of the UV light can be associated with the ejection of the electrons from the metal to the adsorbed oxygen which increases the field across the oxide film.

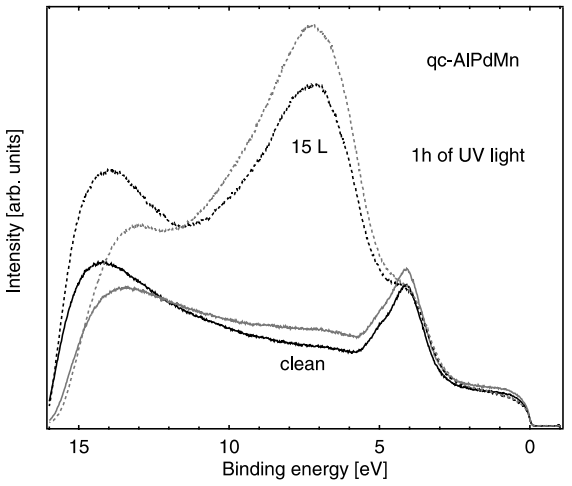

Fig. 5. UPS valence band spectra of the qc-Al–Pd–Mn before (black) and after (grey) 1 h of exposure to UV light. Full lines stand for clean, dashed for surfaces exposed to 15 L of oxygen.

They conclude that it is necessary that the thickness of the oxide layer is larger than 10 Å for this effect to prevail the tunnelling of the electrons back to the metal. In the case of the quasicrystalline surface, this thickness is certainly not exceeded [7,8]. The observed phenomenon could be explained by an increase of diffusivity induced by photon irradiation. On the other hand, the stronger reaction of the previously oxidised surfaces, by comparison to the clean ones, is along the conclusions from Cabrera and Mott [39], where photoelectrons promote the reaction with oxygen across the existing oxide layer.

3.4. LEED

The LEED pattern of Al(1 1 1) consists of three stronger and three weaker spots in hexagonal symmetry. LEED images of qc-Al–Pd–Mn are fivefold symmetric. The clean-surface diffraction spots decline in intensity upon exposure to oxygen until they disappear completely (not shown). No new structure is observed. The disappearance of the diffraction pattern occurs between 7 and 25 L exposure on qc-Al–Pd–Mn, consistent with the results of others [7]. At 75 L exposure only three spots of the six-dots pattern on Al(1 1 1) remain visible. The obliteration of the pattern was not achieved with exposures up to 375 L, but the development of the intensities suggests that it may be expected around 1000 L.

4. Conclusion

Our results can be interpreted in terms of the layer-by-layer surface composition of quasicrystalline Al–Pd–Mn proposed by Gierer et al. [26,27]. The topmost layer of the quasicrystalline Al–Pd–Mn is Al-rich and therefore Al oxidises first. A passivating layer of Al-oxide forms on top and acts as a barrier between oxygen and other elements of the alloy. Mn is present at the surface only in traces, and together with the passivating Al-oxide, this is the reason why we do not observe oxidation of Mn up to very high exposures. Perhaps better statistics, i.e., higher photon flux, would reveal that Mn is slightly oxidised even at

low exposures. Pd appears deeper below the surface and the measurements imply that it is either slightly oxidised or that it reacts to the changes of the environment which is oxidising. The quasicrystalline surface termination plays an important role in the oxidation process. The diffusivities of the elements in the quasicrystal are much smaller than in the elemental samples [35], and so the topmost layer composition determines which elements are oxidising. Some previous works [40,41] suggested that a reduced density of states near the Fermi level might be responsible for less available electrons and thus limited reactivity of quasicrystals. We observe stronger oxidation of the quasicrystal, than of elemental aluminium, which does not relate to their respective densities of states near the Fermi level.

The crystalline phase of the Al–Pd–Mn alloy reacts more with oxygen than the quasicrystalline. The oxidation process saturates at approximately 40 L on the quasicrystalline surface and at 75 L on the crystalline, in both XPS and UPS. There are several factors influencing the observed behaviour. The structure of the crystalline phase is periodic and there is no Al-dense surface layer, which makes all elements available at the surface for oxidation. The morphology of the surface created in the sputtering treatment is rough, favouring rapid and penetrating oxidation. Finally, the diffusivities of the elements are larger than in the quasicrystalline phase. The weak reaction of Pd here can be attributed to its inherent inertness [8]. However, the crystalline phase is less sensitive to UV light or X-rays than the quasicrystalline. This could be the consequence of the photon-induced increase of diffusivities in the quasicrystalline surface.

The quasicrystalline surface is more reactive and more sensitive than Al(1 1 1). The saturation of the oxidation seems to be the same for both surfaces, but the highly reactive Al–Pd–Mn surface achieves this state almost immediately, while the process lasts longer for Al(1 1 1). This suggests that the quasicrystal, in the reactivity, is situated between the Al(1 1 1) surface and other, more reactive, low-index Al faces. Thus, the geometry of the quasicrystalline surface appears more open than the densely packed Al(1 1 1) surface, consistent with the results for the *i*-Al–Pd–Mn surface by Gierer et al. [26,27] and less open than other low-index Al faces.

Upon oxidation the quasicrystals show a particular behaviour such as selective oxidation of their components and formation of a passivating layer, desirable for applications. Furthermore, the observations of the oxidation process allow us to draw conclusions about the quasicrystals surface properties, and to compare them with other materials which are well known.

Acknowledgements

We wish to thank Y. Calvayrac (CECM-CNRS, Vitry-sur-Seine, France) for providing the monograin quasicrystal and T. Greber and J. Osterwalder (University of Zürich) for fruitful discussions. Skilful technical assistance was provided by O. Raetzo, E. Mooser, R. Schmid, O. Zosso, Ch. Neururer and F. Bourqui. This project has been funded by the Fonds National Suisse pour la Recherche Scientifique.

References

[1] C. Janot, Quasicrystals: A Primer, second ed., Oxford University Press, Cambridge, 1994.
[2] J.-M. Dubois, Phys. Scr. T 49 (1993) 17.
[3] C.J. Jenks, P.A. Thiel, Langmuir 14 (1998) 1392.
[4] D. Naumović, P. Aebi, L. Schlapbach, C. Beeli, T.A. Lograsso, D.W. Delaney, Phys. Rev. B 60 (1999) R16330.
[5] B. Bolliger, M. Erbudak, A. Hensch, D.D. Vvedensky, Mat. Sci. Eng. A 294–296 (2000) 859.
[6] D. Naumović, P. Aebi, L. Schlapbach, C. Beeli, Mat. Sci. Eng. A 294–296 (2000) 882.
[7] S.-L. Chang, W.B. Chin, C.-M. Zhang, C.J. Jenks, P.A. Thiel, Surf. Sci. 337 (1995) 135.
[8] S.-L. Chang, J.W. Anderegg, P.A. Thiel, J. Non-Cryst. Solids 195 (1996) 95.
[9] P.J. Pinhero, S.-L. Chang, J.W. Anderegg, P.A. Thiel, Phil. Mag. B 75 (1997) 271.
[10] C.J. Jenks, P.J. Pinhero, S.-L. Chang, J.W. Anderegg, M.F. Besser, D.J. Sordelet, P.A. Thiel, in: A.I. Goldman, D.J. Sordelet, P.A. Thiel, J.M. Dubois (Eds.), Proceedings of the Conference, New Horizons in Quasicrystals: Research and Applications, World Scientific, Singapore, 1997, p. 157.
[11] C.J. Jenks, P.J. Pinhero, T.E. Bloomer, J.W. Anderegg, P.A. Thiel, in: S. Takeuchi, T. Fujiwara (Eds.), Proceed-

ings of the 6th International Conference on Quasicrystals, World Scientific, Singapore, 1998, p. 761.
[12] P.A. Thiel, A.I. Goldman, C.J. Jenks, in: Z.M. Stadnik (Ed.), Physical Properties of Quasicrystals, Springer, Berlin, 1999, p. 327.
[13] B.I. Wehner, U.Köster, in: A.I. Goldman, D.J. Sordelet, P.A. Thiel, J.M. Dubois (Eds.), Proceedings of the Conference, New Horizons in Quasicrystals: Research and Applications, World Scientific, Singapore, 1997, p. 152.
[14] D. Rouxel, M. Gavatz, P. Pigeat, B. Weber, in: A.I. Goldman, D.J. Sordelet, P.A. Thiel, J.M. Dubois (Eds.), Proceedings of the Conference, New Horizons in Quasicrystals: Research and Applications, World Scientific, Singapore, 1997, p. 173.
[15] M. Gavatz, D. Rouxel, D. Claudel, P. Pigeat, B. Weber, in: S. Takeuchi, T. Fujiwara (Eds.), Proceedings of the 6th International Conference on Quasicrystals, World Scientific, Singapore, 1998, p. 765.
[16] C. Berg, S. Raaen, A. Borg, J.N. Andersen, E. Lundgren, R. Nyholm, Phys. Rev. B 47 (1993) 13063.
[17] S.M. Bedair, H.P. Smith Jr., J. Appl. Phys. 42 (1971) 3616.
[18] I.P. Batra, L. Kleinman, J. Electron Spectrosc. Rel. Phenom. 33 (1984) 2175.
[19] S.A. Flodstrom, C.W.B. Martinsson, R.Z. Bachrach, S.B.M. Hagström, R.S. Bauer, Phys. Rev. Lett. 40 (1978) 907.
[20] C.F. McConville, D.L. Seymour, D.P. Woodruff, S. Bao, Surf. Sci. 188 (1987) 1.
[21] H.F. Brune, J. Wintterlin, J. Trost, G. Ertl, J. Wiechers, R.J. Behm, J. Chem. Phys. 99 (1993) 2128.
[22] S.A. Flodstrom, R.Z. Bachrach, R.S. Bauer, S.B.M. Hagström, Phys. Rev. Lett. 37 (1976) 1282.
[23] W. Eberhardt, F.J. Himpsel, Phys. Rev. Lett. 42 (1979) 1375.
[24] R.Z. Bachrach, G.V. Hansson, R.S. Bauer, Surf. Sci. 109 (1981) L560.
[25] H.D. Ebinger, J.T. Yates Jr., Phys. Rev. B 57 (1998) 1976.
[26] M. Gierer, M.A. Van Hove, A.I. Goldman, Z. Shen, S.-L. Chang, C.J. Jenks, C.-M. Zhang, P.A. Thiel, Phys. Rev. Lett. 78 (1997) 467.
[27] M. Gierer, M.A. Van Hove, A.I. Goldman, Z. Shen, S.-L. Chang, P.J. Pinhero, C.J. Jenks, J.W. Anderegg, C.-M. Zhang, P.A. Thiel, Phys. Rev. B 57 (1998) 7628.
[28] C. S. Fadley, in: R.T. Bachrach (Ed.), Synchrotron Radiation Research: Advances in Surface Science, vol. 1, Plenum, New York, 1990.
[29] Th. Pillo, L. Patthey, E. Boschung, J. Hayoz, P. Aebi, L. Schlapbach, J. Electron. Spectrosc. Rel. Phenom. 97 (1998) 243.
[30] S. Doniach, M. Šunjić, J. Phys. C 3 (1970) 285.
[31] B.R. Strohmeier, Surf. Interf. Anal. 15 (1990) 51.
[32] L. Schlapbach, S. Hüfner, S. Büchler, T. Riesterer, J. Less-Common Met. 130 (1987) 301.
[33] M. Boudard, M. de Boissieu, C. Janot, G. Heger, C. Beeli, H.U. Nissen, H. Vincent, R. Ibberson, M. Audier, J.M. Dubois, J. Phys. C 4 (1992) 10149.
[34] M. de Boissieu, unpublished.
[35] P. Archambault, C. Janot, MRS Bulletin 22 (11) (1997) 48.
[36] J.M. Dubois, S.S. Kang, P. Archambault, B. Colleret, J. Mater. Res. 8 (1) (1993) 38.
[37] D.W. Wagman, W.H. Evans, V.B. Parker, R.H. Schumm, I. Halow, S.M. Bailey, K.L. Churney, R.L. Nutall, J. Phys. Chem. Ref. Data 11 (Suppl. 2) (1982) 392.
[38] H. Lüth, Surfaces and Interfaces of Solids, Springer, Germany, 1993.
[39] N. Cabrera, N.F. Mott, Rep. Prog. Phys. 12 (1948) 163.
[40] A.I. Goldman, J.W. Anderegg, M.F. Besser, S.-L. Chang, D.W. Delaney, C.J. Jenks, M.J. Kramer, T.A. Lograsso, D.W. Lynch, R.W. McCallum, J.E. Shield, D.J. Sordelet, P.A. Thiel, American Scientist 84 (1996) 230.
[41] B.I. Wehner, U. Köster, in: S. Takeuchi, T. Fujiwara (Eds.), Proceedings of the 6th International Conference on Quasicrystals, World Scientific, Singapore, 1998, p. 773.